RM No. L7B19

RESEARCH MEMORANDUM

RESULTS OF FLIGHT TESTS AT SUPERSONIC SPEEDS TO DETERMINE THE EFFECT OF BODY NOSE FINENESS RATIO ON BODY AND WING DRAG

By

Ellis R. Katz

Langley Memorial Aeronautical Laboratory
Langley Field, Va.

CLASSIFIED DOCUMENT

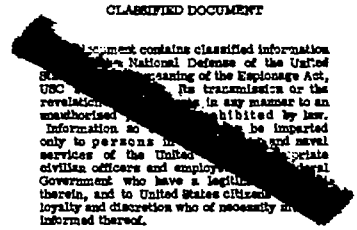

NATIONAL ADVISORY COMMITTEE FOR AERONAUTICS

WASHINGTON

June 26, 1947

Classification cancelled (or changed to UNCLASSIFIED)

By (authority) NASA Tech Pub Announcement #231 - 2 Dec 53
(OFFICER AUTHORIZED TO CHANGE)

By .....

.....
GRADE OF OFFICER MAKING CHANGE)

12 Apr 61
DATE

NACA RM No. L7B19

[redacted]

NATIONAL ADVISORY COMMITTEE FOR AERONAUTICS

RESEARCH MEMORANDUM

RESULTS OF FLIGHT TESTS AT SUPERSONIC SPEEDS TO DETERMINE THE EFFECT OF BODY NOSE FINENESS RATIO ON BODY AND WING DRAG

By Ellis R. Katz

SUMMARY

Flight tests of rocket-powered models at supersonic speeds have been made to determine the effect of nose fineness ratio of winged bodies on total and component drag at high Mach numbers. Wingless models of three nose fineness ratios and winged models of two nose fineness ratios were flown through a Mach number range up to 1.4. On the winged models, each nose fineness ratio was investigated with wings of 45° sweepback and also with unswept wings. Both wings were untapered and of 2.7 aspect ratio. Within the scope of the tests, the results indicated that, with increasing fineness ratio of the nose of a winged body, both the total and wing drag increased at Mach numbers near 1.0 but decreased at higher Mach numbers. For a body alone, however, increasing the nose fineness ratio decreased the body drag. The tests show that the values of wing drag derived in the presence of one body may prove markedly different from those derived from the same wing on a body of different shape.

INTRODUCTION

Flight tests for the evaluation of wing drag have been performed by the Langley Pilotless Aircraft Research Division at its testing station at Wallops Island, Va., with rocket-propelled test models at supersonic speeds. Drag data were reduced from the deceleration of the models through a Mach number range from 1.4 to 1.0. The Reynolds number was approximately 5×10^6 based on wing chord. Reference 1 presents results which are a part of the investigation. The wing drag reduced from these tests, however, is the incremental drag resulting from the addition of a wing to a body-tail configuration. This increment of drag contains not only the pure drag of the wing but also contains interference effects arising from

[redacted]

wing-body interaction phenomena. Throughout the text of this paper, the incremental drag discussed above will be defined as "wing drag." A number of previous reports, typified by reference 1, have presented wing drag obtained from flight tests of winged models all having bodies of identical shape. In order to determine what effect a change in the shape of the body of a winged model might have on wing drag, a series of tests have been conducted on winged models of different body nose fineness ratios.

MODELS AND TESTS

A photograph of a typical winged test model is shown in figure 1. The all-wooden bodies are approximately 5 feet long and of 5-inch diameter. The fuselage is made hollow to accommodate the standard 3.25-inch-diameter Mk. 7 rocket motor which develops 2200 pounds of thrust for 0.87 second at an ambient preignition temperature of 69° F. The stabilizing fins are rotated 45° out of the plane of the wings.

The seven configurations which have been tested are shown in figure 2. The three basic nose shapes are indicated as nose A, nose B, and nose C. Nose A has a blunt nose of 1.94-inch radius; nose B has a sharp nose of fineness ratio 3.5, the profile of which is the median of a conical and a circular arc profile; and nose C has a long sharp nose of fineness ratio 7 derived by multiplying the axial coordinates of profile B by a factor of 2. The untapered wings of all winged configurations were of 2.7 aspect ratio (based on total span and area) and of 0° and 45° sweepback. The NACA 65-009 airfoil sections were maintained normal to the leading edges. All wings had their centers of exposed area located on the bodies 3.4 diameters to the rear of the base of the nose. The location of the wing leading edge on the center line of the body is given by station L in the table in figure 2.

The experimental data were obtained by launching the body at an angle of 75° to the horizontal and determining its velocity along the nearly straight-line flight path. The velocity determination is made possible by a CW Doppler radar unit (AN/TPS-5) located at the point of launching. Two models of each configuration were tested and the results of each are presented. Two additional models of configuration number 3 were flown to extend the Mach number range. A typical time history of flight velocity is shown in figure 3. The deceleration due to drag is determined by graphically differentiating the coasting (after burnout) flight part of the velocity-time curve and subtracting $g \sin \theta$, where g is the acceleration of gravity and θ is the launching angle.

Drag is obtained by multiplying the acceleration values by a factor equal to the ratio of the model weight to the acceleration of gravity. The drag coefficient C_D is derived from the general formula

$$C_D = \frac{D}{\frac{1}{2}\rho S V^2}$$

where D is the drag at the velocity V. The density ρ is determined from altitude–density soundings made prior to the firings. The symbol S is taken as the basic–body frontal area (0.1364 sq ft).

RESULTS AND DISCUSSION

As a means to determine the uniformity of the test results, five wingless test bodies of nose type B have been flown and the values of drag, corrected to standard conditions, are plotted against velocity in figure 4. The maximum experimental scatter from the mean–faired curve appears to be approximately ±10 pounds drag and is nearly constant with velocity. A statistical analysis of figure 4 made by personnel of the Langley Aircraft Loads Division indicated the following probabilities:

(a) In 95 cases out of 100, comparable groups of five models will show no greater scatter than shown in figure 4.

(b) In 95 cases out of 100, the mean curve for groups of five models, two models, or one model will fall within ±2, ±3½, or ±4½ pounds, respectively, of the mean curve of figure 4.

This study dealt only with the standard wingless body and, thus, the results are directly applicable to drag data from exactly similar bodies. The standard practice of firing two test models of each configuration, however, has resulted in only one case in which the scatter was greater than that shown in figure 4, and the average scatter for all cases was about that of figure 4. Thus, the accuracy data presented here may be considered applicable to all configurations tested. The scatter is probably attributable to model fabrication tolerances, instrumentation errors, and errors inherent in the method of data reduction.

[redacted]

Figure 5 shows drag coefficient plotted against Mach number for all models of each configuration tested, with the exception of configuration number 6 which has been presented in reference 2. Faired curves have been drawn as the median of each set of models and these curves are used as the basis for the following discussion.

Total Drag

The curves of total drag coefficient for the nose B and the nose C winged bodies of 0° and 45° sweepback are presented in figure 6. At Mach numbers near 1.0, greater drag coefficients are evidenced for the winged body with nose C than with the blunter nose B; but the reverse is true at the higher Mach numbers. This reversal of effect occurs at a lower Mach number for the unswept wing than for the swept wing. It appears, therefore, that the effect of sweepback is to increase the Mach number at which the total drag coefficient will decrease with an increase in nose fineness ratio.

Body Drag

Figure 7 shows curves of body drag coefficient (fins included) for bodies with noses A, B, and C. The curves indicate that above a Mach number of approximately 1.05 body drag coefficient decreases with increasing nose fineness ratio and that the effect increases with Mach number. The reversal of effect at Mach numbers near 1.0 is presently inexplicable and will bear further investigation. At a Mach number of 1.3, the drag coefficient of the blunt nose A model is decreased approximately 26 and 30 percent by increasing the nose fineness ratio to that of the nose B and nose C models, respectively.

Wing Drag

Figure 8 shows the variation of wing drag coefficient with Mach number for two values of sweepback, 0° and 45°, and for two nose types, nose B and nose C. The values of wing drag coefficient are derived as the difference between the drag coefficients for a winged and wingless model of the same nose type, and the values include possible interference effects. The wings of 0° and 45° sweep show greater drag with nose C than with the blunter body nose B at Mach numbers close to 1.0. As the Mach number increases, however, the effect decreases for the swept wing and reverses in the case of the unswept wing. Thus, sweepback increased the value of the Mach number at which wing drag coefficient decreases with increasing nose fineness ratio.

Examination of the wing-drag-coefficient curves reveals that, throughout the Mach number range, sweepback provided a greater drag reduction on the blunter B-nosed configuration than on the sharper C-nosed configuration. For Mach numbers between 1.1 and 1.25, 45° of sweep resulted in approximately 70- and 60-percent drag reduction for the short- and long-nosed configurations, respectively.

CONCLUSIONS

Within the scope of the tests, the following conclusions were noted:

1. Values of wing drag derived in the presence of one body proved markedly different from those derived from the same wing on a body of different shape.

2. For the winged configurations, an increase in the body nose fineness ratio resulted in an increase of total drag coefficient near Mach numbers of 1.0 but resulted in a decrease of drag coefficient at higher Mach numbers. Wing sweep increased the Mach number at which the reversal of effect occurs.

3. For the winged configurations, an increase in the body nose fineness ratio resulted in an increase of wing drag coefficient for swept and unswept wings near Mach numbers of 1.0. At the higher Mach numbers, the effect decreased for the swept wing and actually reversed for the unswept wing.

4. For the winged configurations, an increase in the body nose fineness ratio decreased the reduction of drag due to sweepback.

5. For the wingless configurations, an increase in the body nose fineness ratio decreased the body drag coefficient.

Langley Memorial Aeronautical Laboratory
National Advisory Committee for Aeronautics
Langley Field, Va.

[redacted]

REFERENCES

1. Alexander, Sidney R., and Katz, Ellis: Drag Characteristics of Rectangular and Swept-Back NACA 65-009 Airfoils Having Aspect Ratios of 1.5 and 2.7 as Determined by Flight Tests at Supersonic Speeds. NACA RM No. L6J16, 1946.

2. Alexander, Sidney R., and Katz, Ellis: Flight Tests to Determine the Effect of Length of a Conical Windshield on the Drag of a Bluff Body at Supersonic Speeds. NACA RM No. L6J16a, 1947.

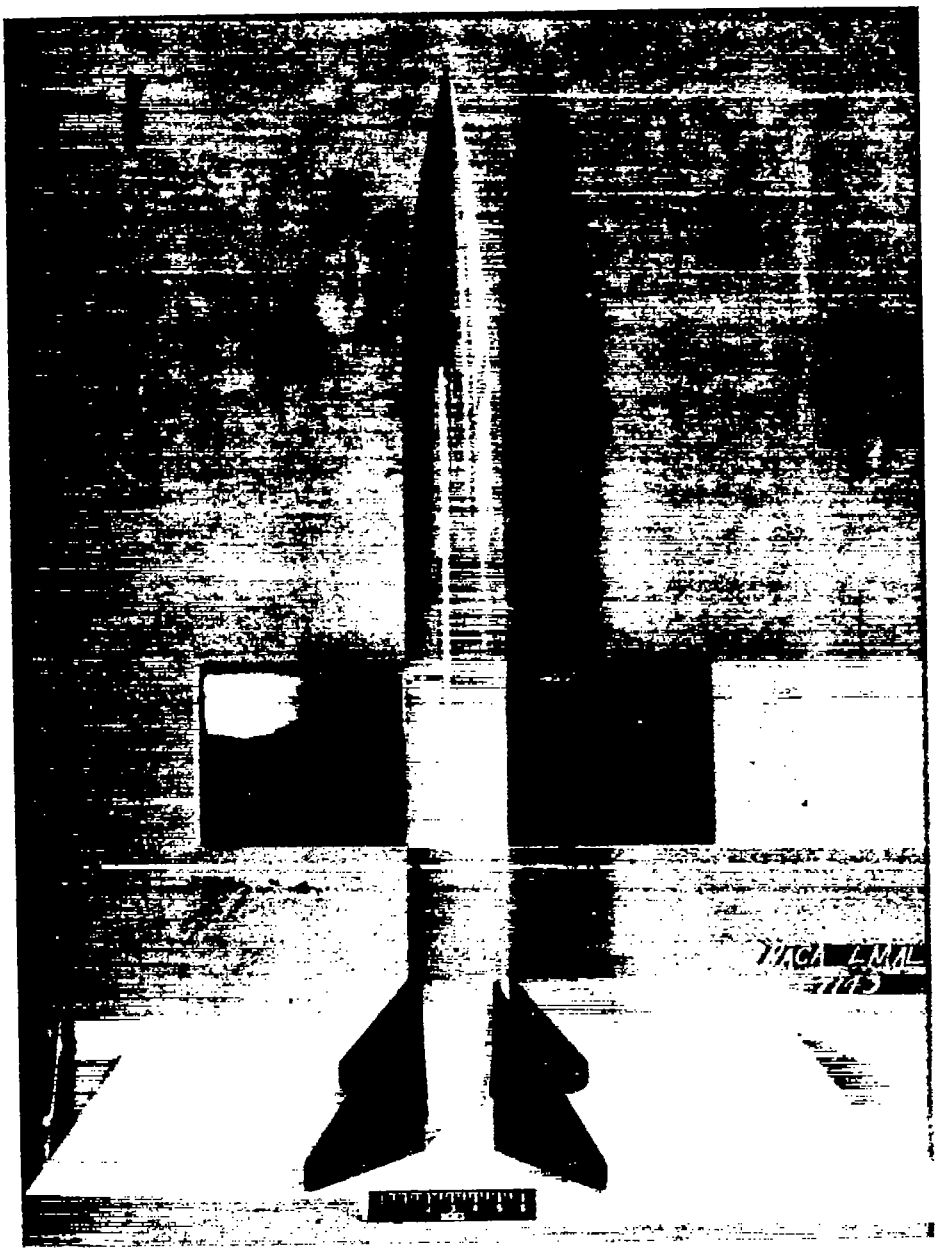

Figure 1.- General arrangement of typical winged test body.

[redacted]

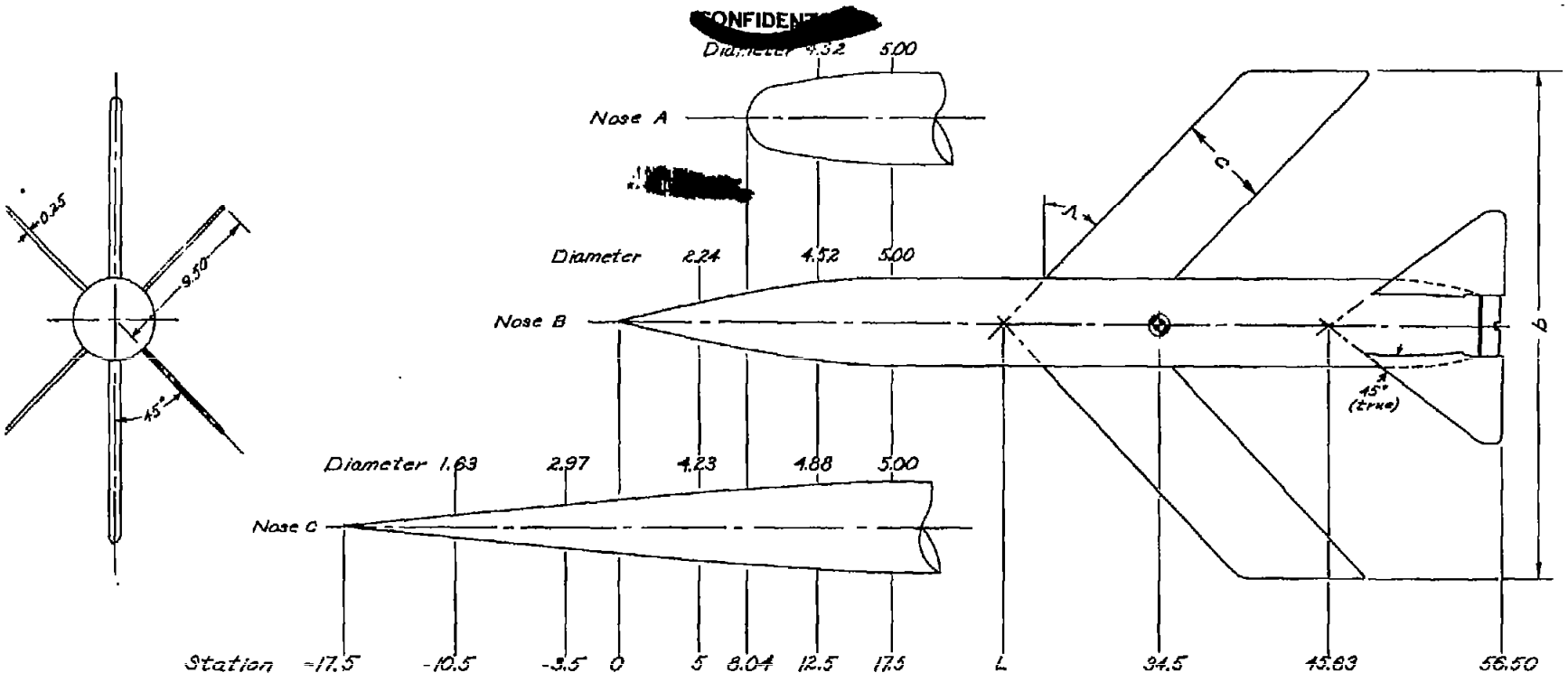

Configuration	Nose	L (in.)	Λ (deg)	b (in.)	c (in.)	Aspect ratio
1	B	32.09	0	25.73	9.65	2.7
2		25.76	45		6.88	
3	C	32.09	0		9.65	
4		25.76	45		6.88	
5	A	Wingless				
6	B					
7	C					

NATIONAL ADVISORY COMMITTEE FOR AERONAUTICS

Figure 2.- General arrangement of test bodies investigated. Wing area (exposed), 200 sq in.; airfoil (normal to L.E.), NACA 65-009, fin area (exposed), 136.5 sq in.; weight (burnt out), 30 lbs approx.

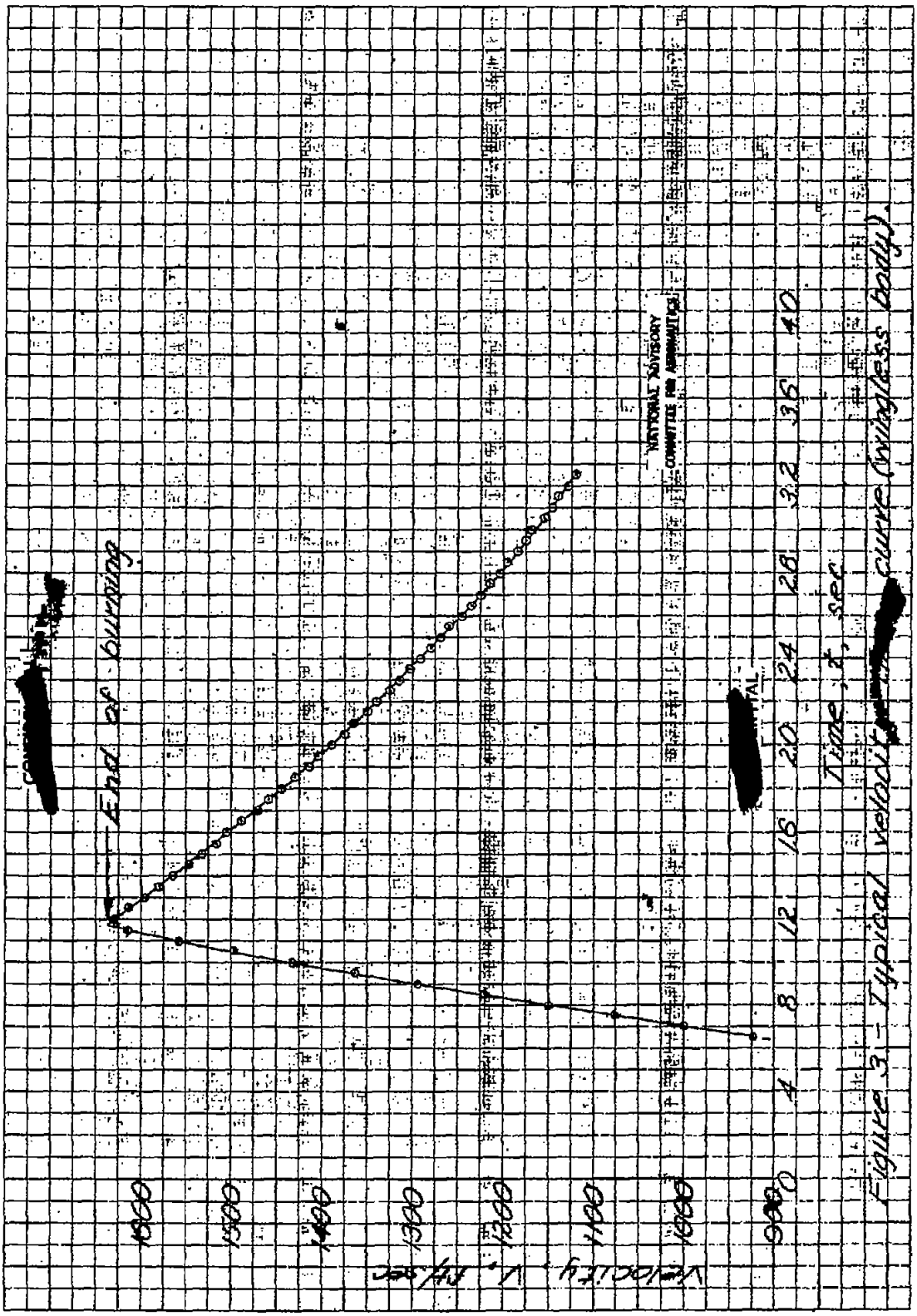

Figure 3.- Typical velocity-time curve (wingless body).

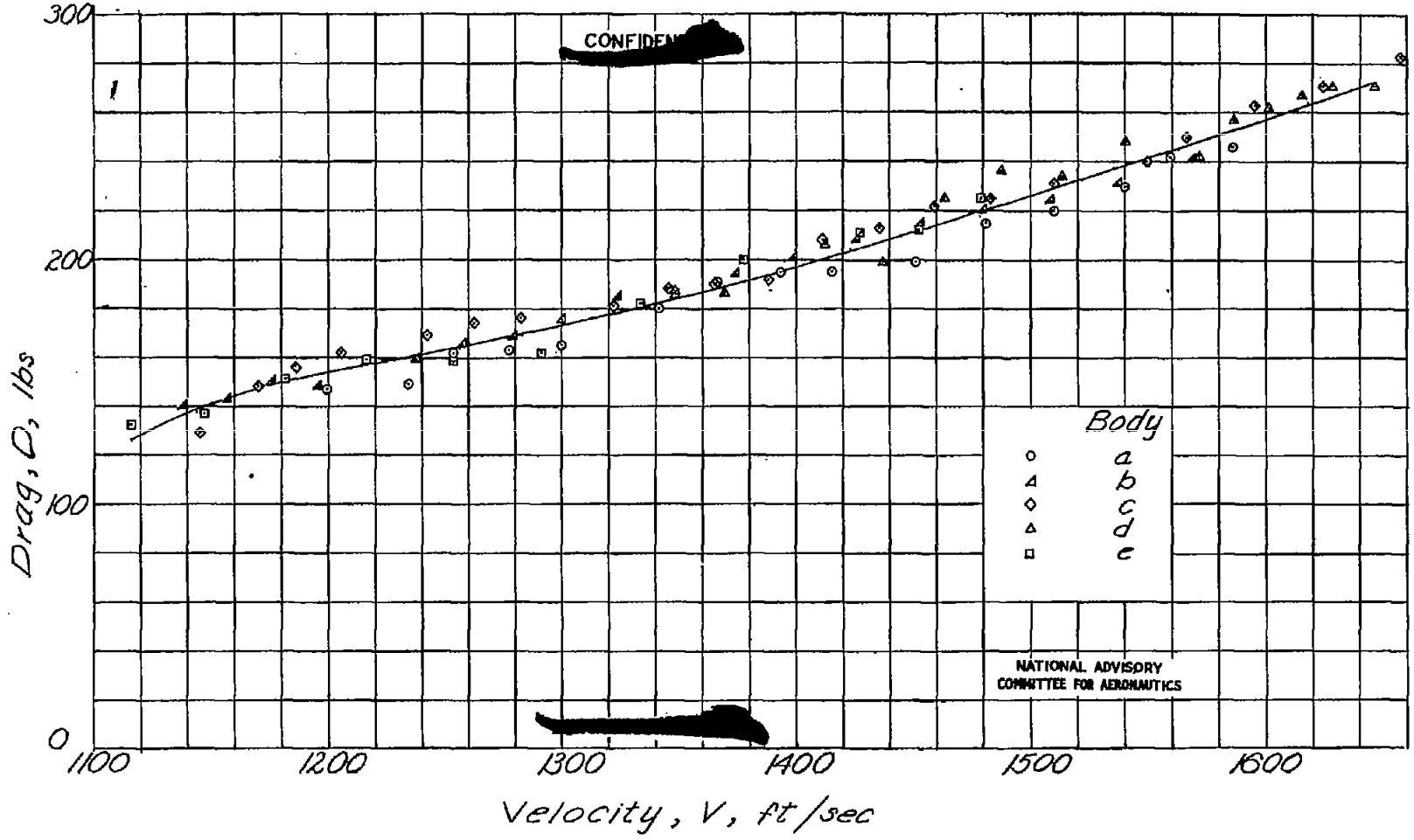

Figure 4.- Drag curves for five wingless bodies of nose shape B reduced to sea-level standard conditions.

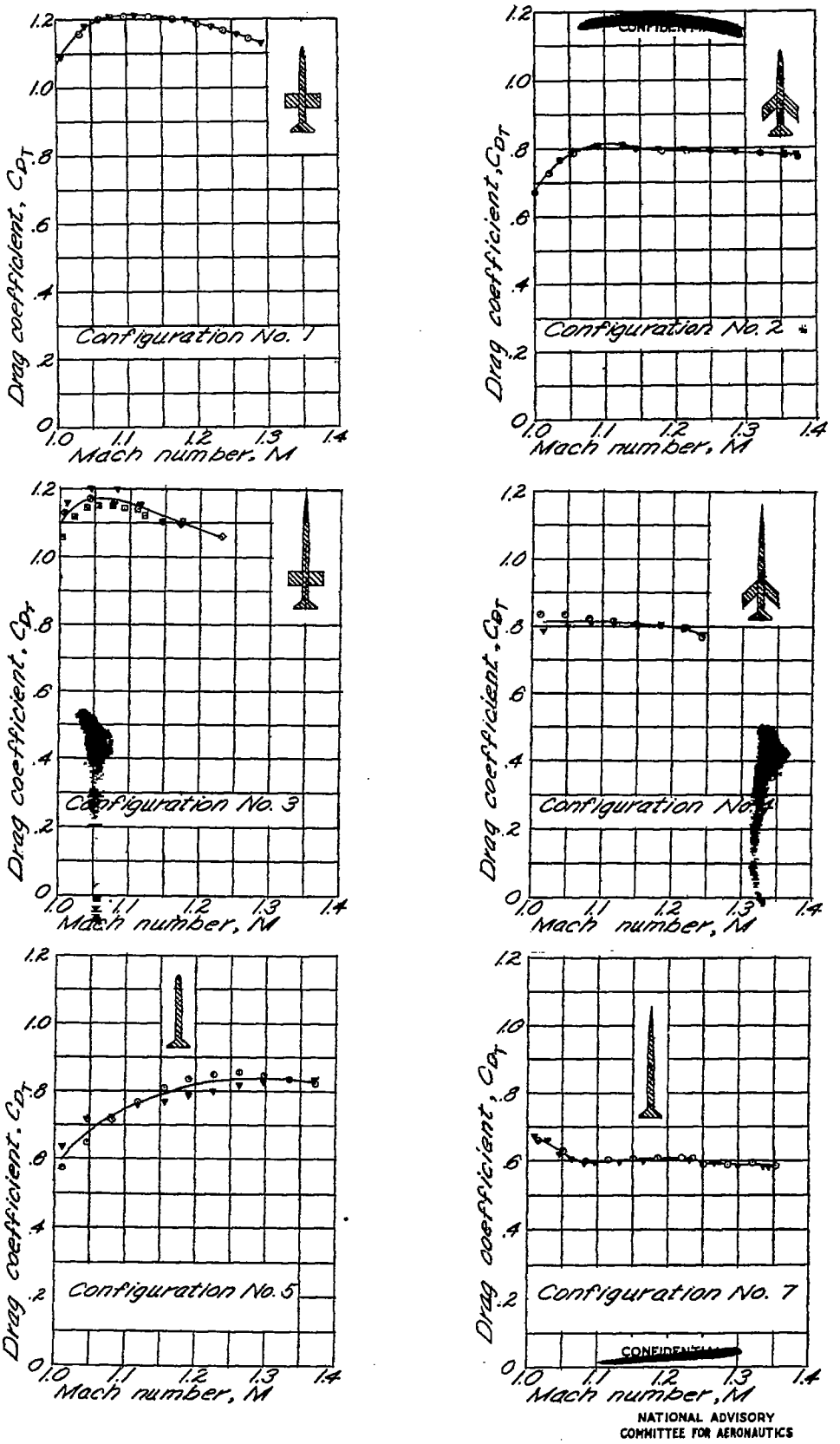

Figure 5. - Drag coefficient data for the models of each configuration tested with exception of No. 6.

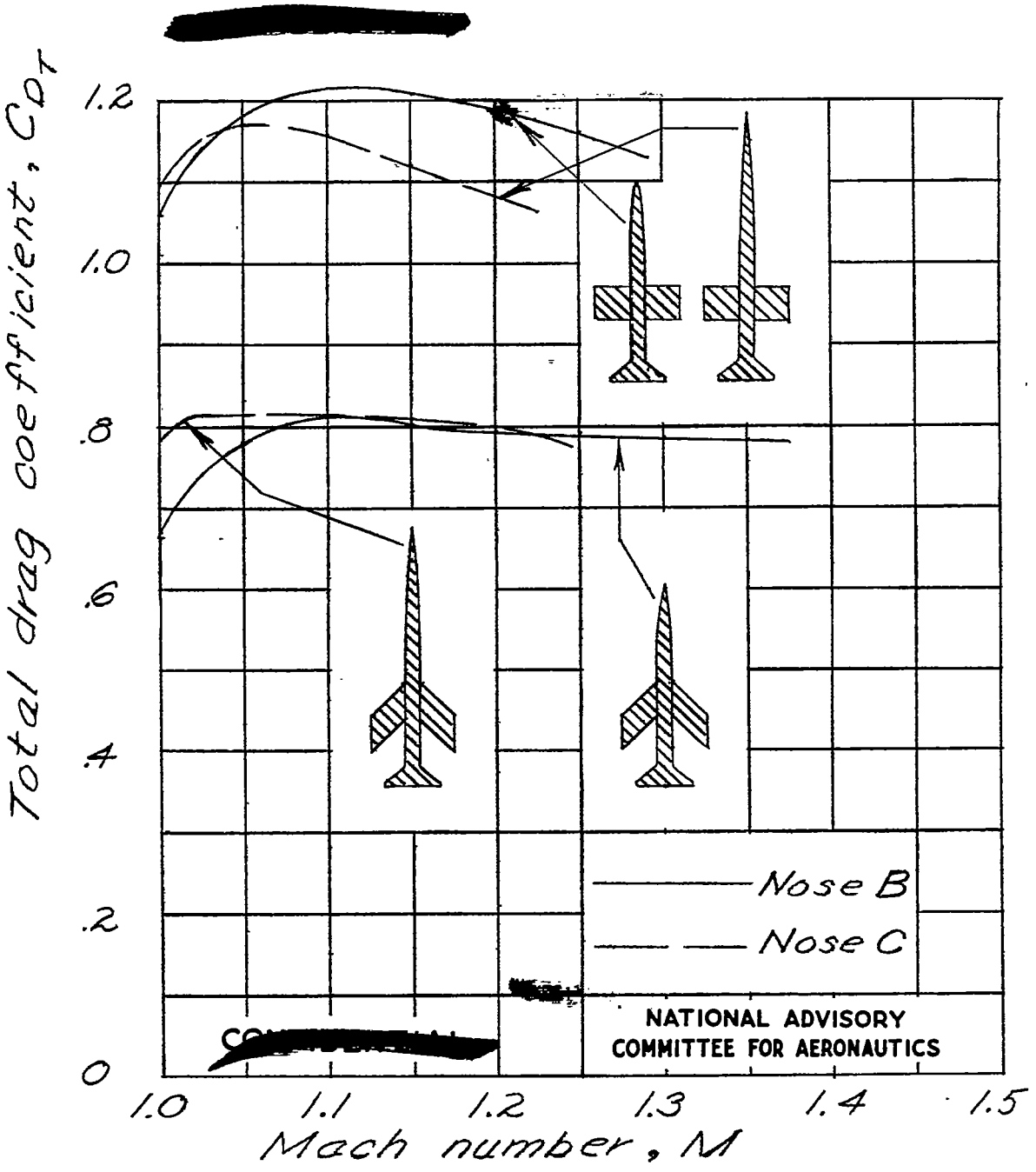

Figure 6.- Total drag coefficient for winged configurations of two nose types with wings of 0° and 45° sweepback, aspect ratio of 2.7.

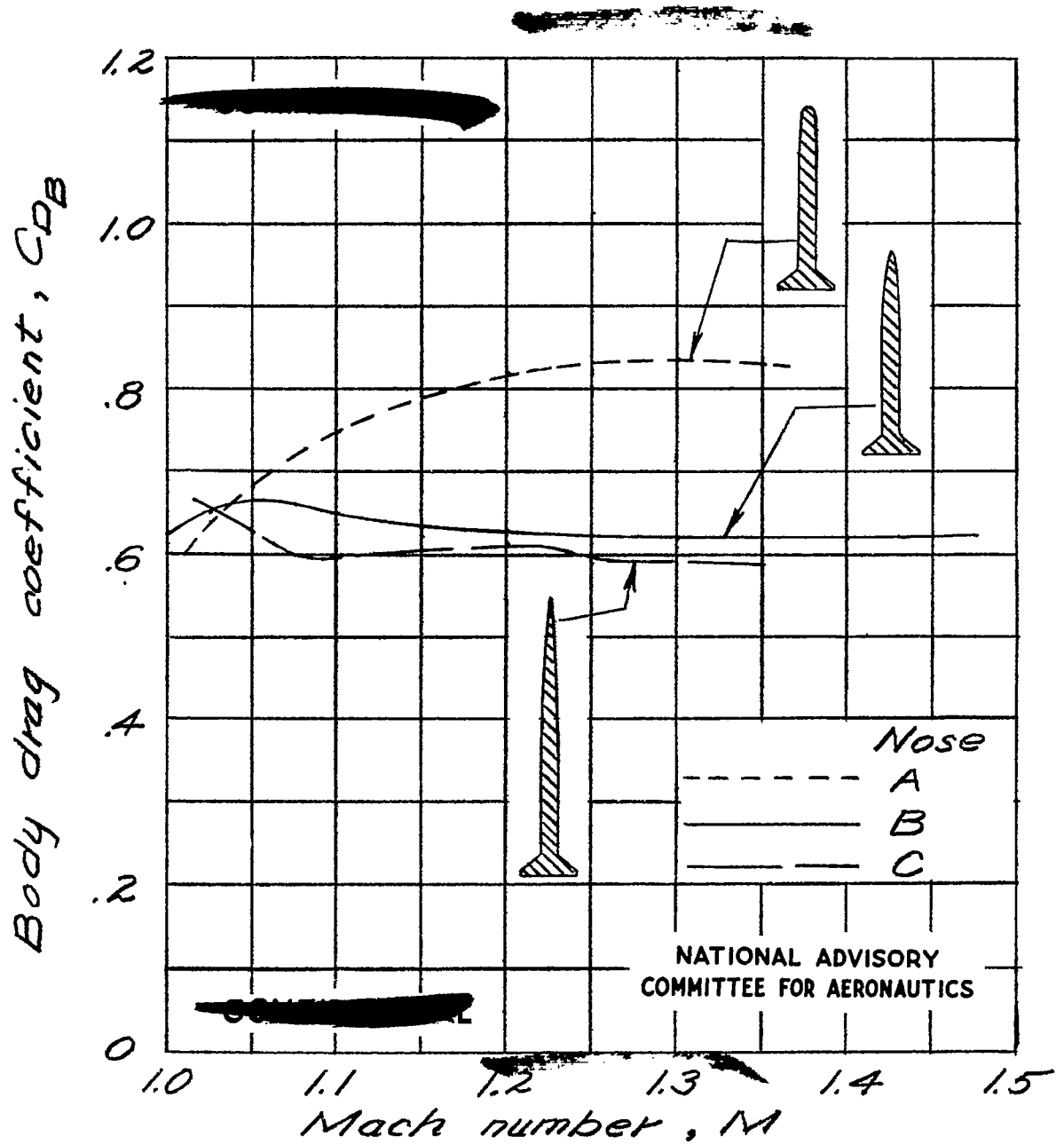

Figure 7.- Body drag coefficient for three nose shapes.

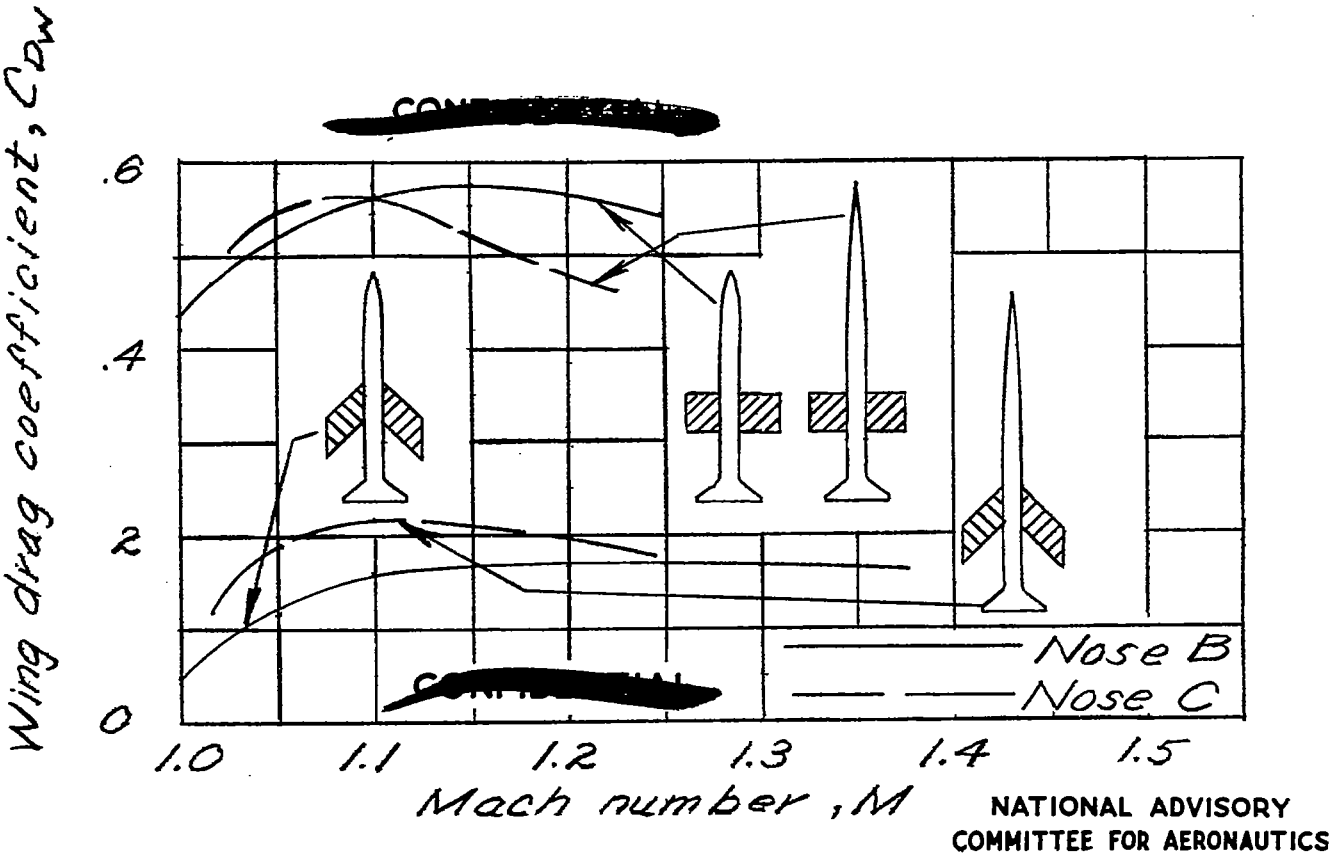

Figure 8.- Wing drag coefficient for wings of 0° and 45° sweepback in presence of bodies of two nose types, aspect ratio of 2.7.